# Artificial intelligence based robust nonlinear controllers optimized by improved gray wolf optimization algorithm for plug-in hybrid electric vehicles in grid to vehicle applications

By

**Shabab Saleem**

NUSTMSEE-2K21-CS00000360680

Supervisor

**Dr. Iftikhar Ahmad**

Department Electrical Engineering

School of Electrical Engineering and Computer Sciences (SEECS)

National University of Sciences and Technology (NUST)

Islamabad, Pakistan , June 2023

# Approval

It is certified that the contents and form of the thesis entitled "Artificial intelligence based robust nonlinear controllers optimized by GWO algorithm for plug-in hybrid electric vehicles in grid to vehicle applications" submitted by Shabab Saleem have been found satisfactory for the requirement of the degree
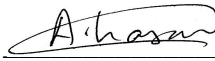
Advisor :   Dr. Iftikhar AHMAD

Signature: _____

Date: _____10-Aug-2023_____

Committee Member 1:Dr. Muhammad Latif Anjum

Signature: _____

11-Aug-2023

Committee Member 2:Dr. Ammar Hasan

Signature: _____

Date: _____16-Aug-2023_____

Signature: _____

Date: _____

# THESIS ACCEPTANCE CERTIFICATE

Certified that final copy of MS/MPhil thesis entitled "Artificial intelligence based robust nonlinear controllers optimized by GWO algorithm for plug-in hybrid electric vehicles in grid to vehicle applications" written by Shabab Saleem, (Registration No 360680), of SEECS has been vetted by the undersigned, found complete in all respects as per NUST Statutes/Regulations, is free of plagiarism, errors and mistakes and is accepted as partial fulfillment for award of MS/M Phil degree. It is further certified that necessary amendments as pointed out by GEC members of the scholar have also been incorporated in the said thesis.

Signature: _____          ____    ____

Name of Advisor: ____Dr. Iftikhar AHMAD____ __

Date: _____10-Aug-2023_____ __

HoD/Associate Dean:_____

Date: _____

Signature (Dean/Principal): _____ ___

Date: _____

# Certificate of Originality

I hereby declare that this submission titled "Artificial intelligence based robust nonlinear controllers optimized by GWO algorithm for plug-in hybrid electric vehicles in grid to vehicle applications" is my own work. To the best of my knowledge it contains no materials previously published or written by another person, nor material which to a substantial extent has been accepted for the award of any degree or diploma at NUST SEECS or at any other educational institute, except where due acknowledgement has been made in the thesis. Any contribution made to the research by others, with whom I have worked at NUST SEECS or elsewhere, is explicitly acknowledged in the thesis. I also declare that the intellectual content of this thesis is the product of my own work, except for the assistance from others in the project's design and conception or in style, presentation and linguistics, which has been acknowledged. I also verified the originality of contents through plagiarism software.

Student Name:Shabab Saleem

Student Signature: _____

**NUST School of Electrical Engineering and Computer Sciences**
*A center of excellence for quality education and research*

**CERTIFICATE**

Certified that the Scrutinizing Committee has reviewed the final documentation of

Mr./Mrs/Miss  Shabab Saleem  Regn No.      360680

Student of  SEECS , NUST thesis title  Artificial intelligence based robust nonlinear controllers

optimized by improved gray wolf optimization algorithm for plug-in hybrid electric vehicles in

grid to vehicle applications and found satisfactory as per NUST's standard format for Master
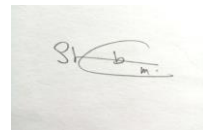
Thesis.

**Supervisor**

**Iftikhar Ahmad**

# Declaration

I, *Shabab Saleem* declare that this thesis titled "Artificial intelligence based robust nonlinear controllers optimized by improved gray wolf optimization algorithm for plug-in hybrid electric vehicles in grid to vehicle applications.

I confirm that:

1. This work was done wholly or mainly while in candidature for a Master of Science degree at NUST

2. Where any part of this thesis has previously been submitted for a degree or any other qualification at NUST or any other institution, this has been clearly stated

3. Where I have consulted the published work of others, this is always clearly attributed

4. Where I have quoted from the work of others, the source is always given. With the exception of such quotations, this thesis is entirely my own work

5. I have acknowledged all main sources of help

6. Where the thesis is based on work done by myself jointly with others, I have made clear exactly what was done by others and what I have contributed myself

Shabab  Saleem,NUSTMSEE-K21-CS00000360680

# Copyright Notice

This thesis is dedicated to *my beloved parents and my supervisor*

*Dr. Iftikhar Ahmed Rana*

# Abstract

The paper introduces a control strategy for a plug-in hybrid electric vehicle (PHEV) system, integrating a photovoltaic-based RES with battery and supercapacitor-based ESS. The objective is to efficiently utilize the PV system using a neural network to determine its maximum power points. To ensure robust control, the paper designs both a robust nonlinear higher-order super twisting sliding mode controller and an integral terminal sliding mode controller.

One notable aspect of the proposed system is the implementation of a current-fed converter for the PV and supercapacitor. Unlike SCR-based converters, current-fed converters prevent device failure and core saturation, making them more reliable. This characteristic contributes to the overall robustness of the system. The integration of the neural network, along with the designed controllers and current-fed converter, enhances the efficiency and reliability of the plug-in hybrid electric vehicle system. This research holds promise for developing advanced and resilient energy management solutions for sustainable transportation systems in the future. Additionally, a power bi-directional converter is employed for the battery in the EV system. This converter enables the battery to both charge and discharge power as required by the system which facilitates the energy flow between the battery and the rest of the system, allowing efficient energy management and utilization within the PHEVs. The integration of ANN for PV with the above mentioned converters and controllers along with improved-gray wolf optimization represents the novelty of this work. The paper confirms global asymptotic stability of the control method using Lyapunov stability analysis. It further demonstrates the proposed system's behavior through a hardware-in-the-loop experiment.

**Keywords:** *PV, SC, Battery, (DC-DC) Current-Fed Bridge Converter, Bi-directional Power Converter, ANN, GWO, HIL, EV's*

# Acknowledgments

I would like to express my deepest gratitude to my thesis advisor [Dr, Iftikhar Ahmed Rana] for their invaluable guidance, support, and expertise throughout the entire research process. Their insightful feedback and constructive criticism have been instrumental in shaping this thesis.

I am immensely grateful to [Syed Hassan Ahmed Shah] , [Rimsha Ghias] and [Atif Rehman ] for their valuable inputs, encouragement, and mentorship. Their scholarly expertise and willingness to share their knowledge have greatly enriched my understanding of the subject matter.

I extend my heartfelt appreciation to the participants of this study who generously contributed their time and insights. Without their cooperation, this research would not have been possible, and I am truly grateful for their involvement.

# Contents

# List of Figures

# List of Tables

# List of Abbreviations and Symbols

## Abbreviations

| | |
|---|---|
| **EV** | Electric Vehicle |
| **PV** | Photovoltaic |
| **SC** | Supercapacitor |
| **EMS** | Energy Mangment System |
| **ANN** | Artificial Neural Network |
| **GWO** | Gray wolf Optimization |
| **HIL** | HardWare in Loop |

CHAPTER 1

# Introduction

## 1.1  Background

Electric vehicles (EVs) are rapidly gaining popularity as a viable alternative to conventional internal combustion engine (ICE) vehicles [1]. This surge in popularity can be attributed to their superior energy efficiency and lack of local pollution, making them an attractive option for mitigating environmental pollution and reducing energy consumption. An essential characteristic of EVs is their significant capacity to store electrical energy, enabling them to contribute to power system control and management.

Photovoltaic (PV) systems are a primary renewable energy source; however, their intermittent nature makes them unreliable without an ESS [2]. To address power imbalances and reduce the size of the ESS, PV systems are often complemented with batteries and SCs. This combination ensures a balanced and efficient power flow in EVs. When renewable energy sources like PV cannot meet energy demands, batteries serve as backup energy sources. Meanwhile, an energy storage and management system, such as a supercapacitor, compensate for power variations during consumption or production. Operating PV systems at their MPP is crucial for optimizing their performance and achieving efficiency [3]. The output power of PV systems is influenced by various environmental factors, including temperature and solar radiation. By ensuring they operate at their MPP, the overall efficiency and effectiveness of PV systems in EVs can be maximized.
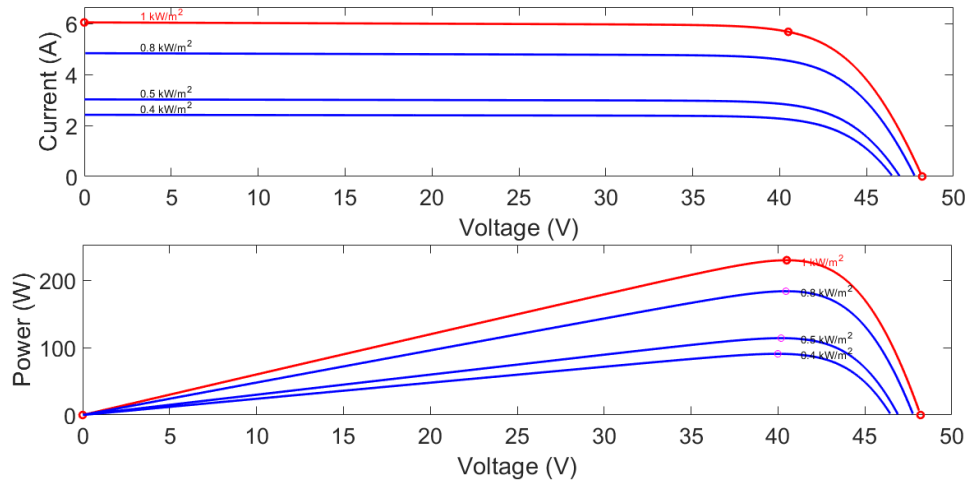
**Figure 1.1:** IV and PV Characteristics of varying Irradiance
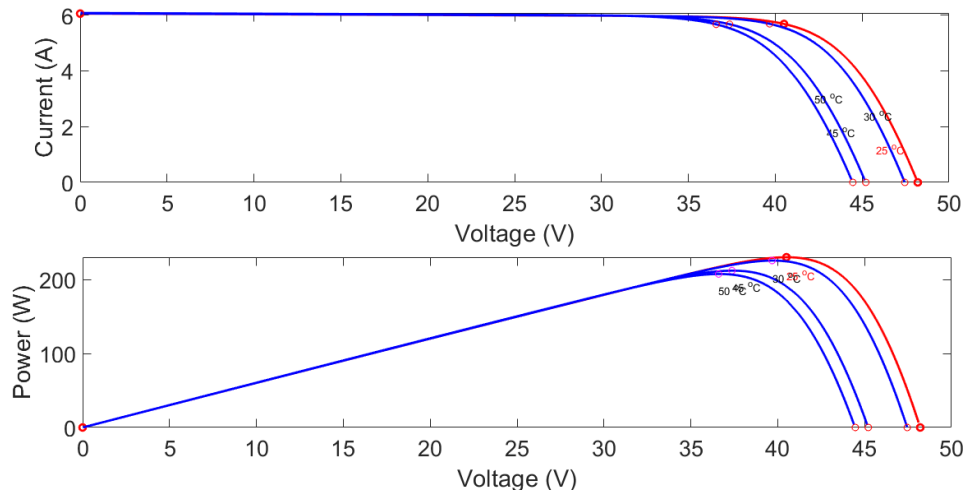


**Figure 1.2:** IV and PV Characteristics of Varying Temperature
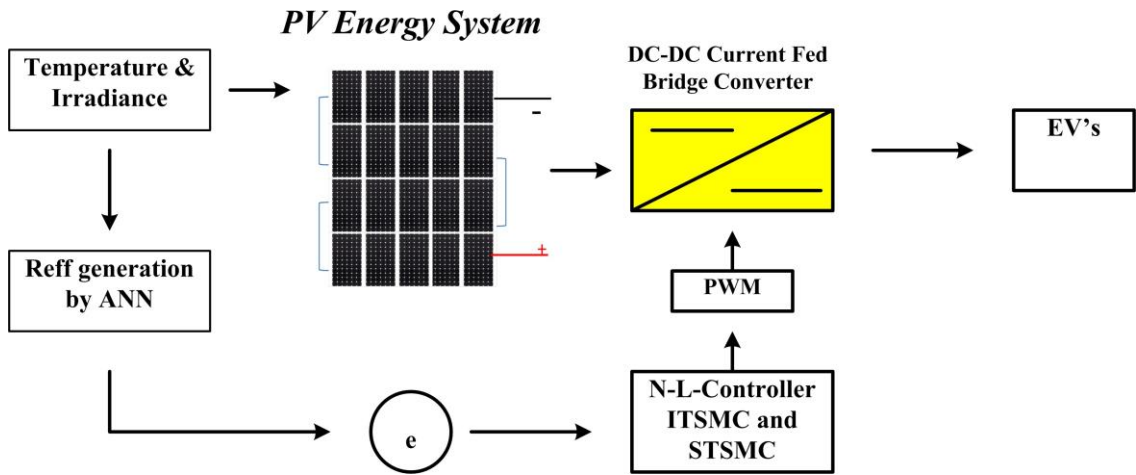
**Figure 1.3:** PV System Strategy

## 1.2 Problem Statment

A solar panel comprises PV modules that convert sunlight into DC electricity through specialized cells. Figure 2 illustrates the PV energy system, wherein the PV array is connected to a DC-DC current-fed bridge converter to facilitate power exchange with the DC bus [4]. Operating in CCM, this converter ensures a consistent and reliable power supply to the electric vehicle. The converter comprises essential components, such as a capacitor Cp, inductor Lp, resistor Rp, and two IGBT switches S1 and S2.

Figure 1.3 showcases the control strategy employed for MPPT of the PV system. Operating photovoltaic (PV) systems at their MPP is crucial for optimal performance. Researchers have extensively studied various MPPT algorithms, including linear and nonlinear controllers, conventional techniques, as well as AI and fuzzy logic-based methods. Among these, AI-based MPPT algorithms have demonstrated greater effectiveness, particularly in handling the unpredictable nature of RESs [5]. These algorithms can adapt to changing conditions more effectively, ultimately enhancing the overall efficiency of PV systems.

# Literature Review

Electric vehicles (EVs) offer a cleaner and more sustainable alternative to conventional vehicles fueled by gasoline or diesel. They rely on electric motors and rechargeable batteries, producing zero emissions at the point of use. By reducing emissions, EVs contribute to improved air quality, climate change mitigation, and decreased reliance on fossil fuels [6]. Additionally, EVs bring benefits such as lower operating costs and higher energy efficiency compared to traditional vehicles. With ongoing technological advancements, the goal is to make EVs even more efficient, reliable, and cost-effective, making them a more viable option for consumers.

The main objective of EVs is to provide a cleaner, more efficient, and sustainable mode of transportation, benefiting both the environment and the people who depend on transportation for their daily needs.

To achieve this, a novel energy management system is introduced, employing artificial neural networks (ANN) to control Renewable Energy Sources (RESs) integrated with Energy Storage Systems (ESS). This system works in tandem with the super-twisting sliding mode control (STSMC) algorithm, known for its capability to handle parametric variations and external disturbances.

The energy management system ensures that the RESs integrated with EVs operate at their maximum power point (MPP), optimizing efficiency throughout the day despite environmental fluctuations that could affect their performance. By incorporating ANN with STSMC, this innovative system effectively manages RESs and ESS, guaranteeing optimal performance and efficiency even in the presence of external disturbances and environmental changes. The combination of these technologies holds promise for
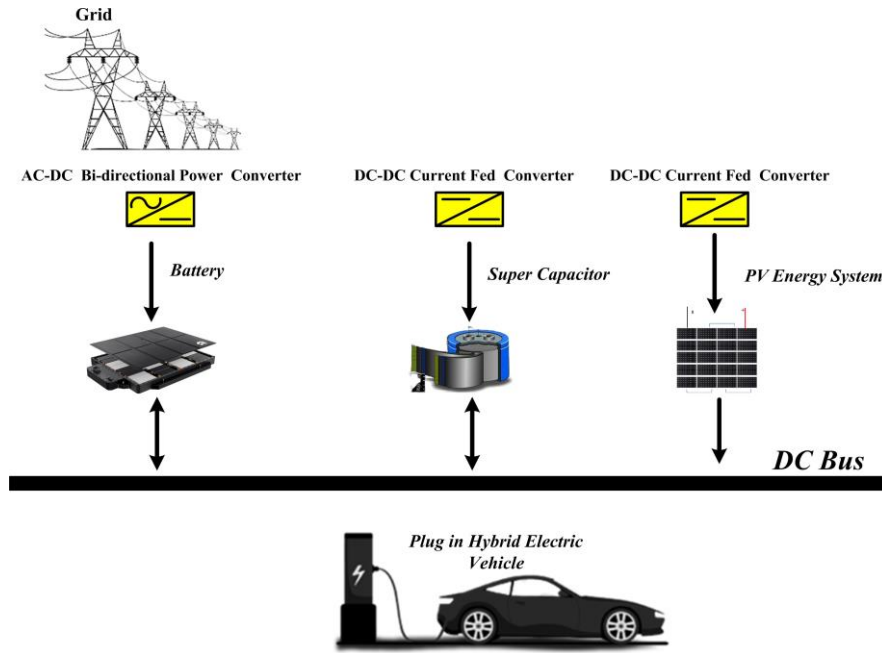
**Figure 2.1:** Block diagram of proposed system

enhancing the overall sustainability and reliability of EVs. [7].

- The study introduces two robust nonlinear controllers, namely the IT-SMC and the ST-SMC, designed to enhance the performance of electric vehicles (EVs). These controllers aim to facilitate smooth EV operations while mitigating disturbances, leading to improved dynamics and extended battery life. Additionally, they effectively minimize the chattering effect, resulting in enhanced system efficiency and reduced power losses.

- To optimize the performance of these controllers, their gains are fine-tuned using a meta-heuristic algorithm called the I-GWO algorithm.

- The main objective of these controllers is to ensure effective management and control of the bidirectional power flow during Vehicle-to-Grid (V2G) or Grid-to-Vehicle (G2V) modes, ensuring seamless integration with the power grid.

- To validate the effectiveness of the system, the study conducts Hardware-in-the-Loop (HIL) and D-Space experiments. These experiments serve as practical tests to confirm the controllers' performance and feasibility in real-world scenarios.

## 2.1   Components

The electric vehicle (EV) consists of several essential components, such as a photovoltaic (PV) array, a supercapacitor (SC), and energy storage systems (ESSs).

## 2.2   Photovoltaic (PV) Array

A solar panel functions as a collection of PV modules, each containing individual cells that harness sunlight and convert it into direct current (DC) electricity. Figure 2.1 illustrates the configuration of the PV energy system. To enable power exchange with the DC bus, the PV array is connected to a DC-DC current-fed bridge converter, as mentioned in reference [8]. This setup efficiently utilizes the generated solar power, thereby enhancing the overall performance of the system.

The converter operates in Continuous Conduction Mode (CCM), ensuring a stable and reliable power supply to the electric vehicle. It comprises a capacitor Cp, inductor Lp, resistor Rp, and two IGBT switches, S1 and S2. This converter plays a crucial role in facilitating smooth power transfer and maintaining the system's integrity during energy conversion.

## 2.3   Supercapacitor  (SC)

Supercapacitors offer a faster and more efficient method for the system to gather energy, leading to reduced stress on batteries and extended overall lifetime while keeping costs to a minimum, as referenced in [9]. Unlike conventional capacitors that store electricity through chemical reactions in a static state, supercapacitors work differently. They employ conducting plates, known as electrodes, separated by an insulating material called a dielectric. When connected to an electric circuit, these plates generate an electrical field that polarizes atoms in the dielectric, creating a charge. This unique mechanism enables supercapacitors to effectively store and release electrical energy as required. The resulting double electric layer attracts opposite polarity electrons in the electrolyte, allowing supercapacitors to store significantly more power than standard capacitors. This capability makes them a valuable component in the system, enhancing energy efficiency and supporting smooth power delivery.

## 2.4   Battery System

The proposed electrical circuit diagram of the EV model is shown in Figure 3.1. It includes an additional bidirectional DC-DC power converter that connects to the EV battery. This converter consists of an inductor (Ld), a capacitor (Cd), and a half-bridge circuit equipped with two switches (S5 and S6). The converter serves as a crucial link between the battery and the DC bus, capable of functioning as either a buck converter or a boost converter depending on the direction of energy flow.

In this study, the electrical battery model incorporates two resistors and one capacitor. To control the converter's switching, a PWM (Pulse Width Modulation) circuit generates switching signals (u1, u2, and u3) with values in the finite set 0, 1, as referenced in [15]. This comprehensive setup ensures efficient power exchange between the battery and the DC bus, enabling the effective operation of the EV model and optimizing its overall performance. This circuit design enhances the EV's energy efficiency and supports seamless power transfer, contributing to a more reliable and efficient electric vehicle system.

## 2.5   Proposed  Methodology

In this thesis, we present robust nonlinear controllers, including fast and non-singular integral terminal sliding mode controllers and super twisting sliding mode controllers. These controllers effectively address the previously mentioned issues and minimize the chattering effect, providing an optimal solution. They generate duty cycles and provide them to converters to ensure proper operation.

The rest of the paper is structured as follows: Chapter 3 describes the energy management scheme and the mathematical modeling of the system. In Chapter 4, we state the controller design objectives and present the design of the two controllers and the ANN-based MPPT algorithm. Chapter 5 showcases the MATLAB/Simulink based simulation results. Finally, Chapter 6 covers the conclusion and outlines future work.

# Proposed Approach and System Modelling

## 3.1   Overview of the system

The proposed electric vehicle (EV) model is depicted in Figure 2.1, illustrating the electrical circuit diagram. The system incorporates three main power sources: PV modules, supercapacitors, and a battery, alongside a capacitor (Cv) responsible for filtering the DC bus voltage. The power converter functions as a boost rectifier in the G2V mode and as an inverter in the V2G mode [8]. The EV model includes a regulation mechanism for the DC bus current (Idc). Alongside this, a bidirectional DC-DC converter is connected to the EV battery, playing a vital role as a link to the DC bus. This converter has the flexibility to operate as either a buck or a boost converter, allowing safe battery discharging in boost mode and efficient battery charging in buck mode. The system is designed to ensure seamless energy exchange between the battery and the DC bus, optimizing overall performance in both modes. This setup guarantees smooth and reliable power flow, contributing to the EV's efficiency and effectiveness in managing energy during different operational scenarios. By regulating the DC bus current and employing a bidirectional converter, the EV model becomes a more versatile and efficient solution for electric transportation.
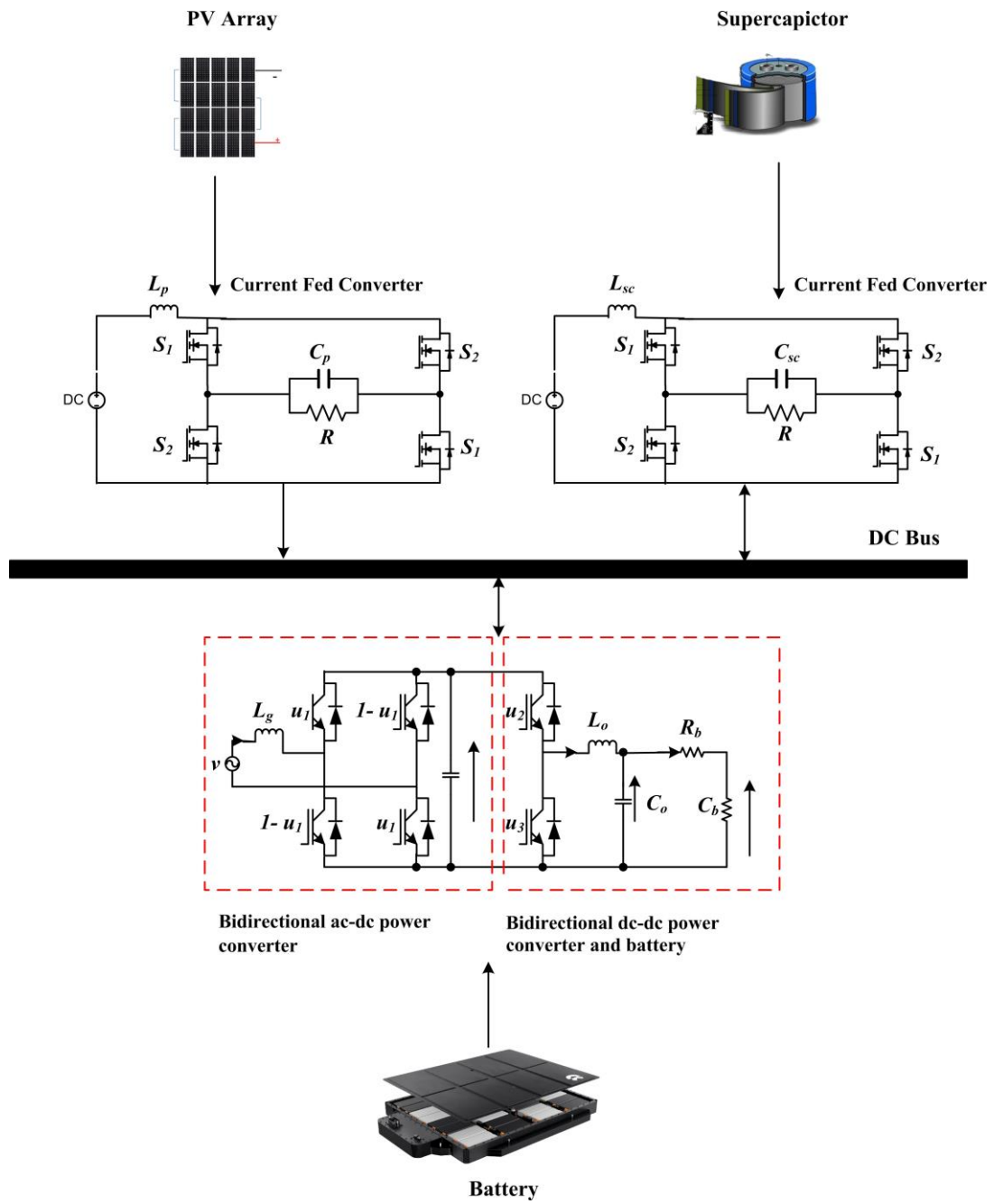
**Figure 3.1:** Circuit diagram of proposed system

## 3.2 Modeling of the System

The integrated model presented in this study encompasses the fundamental aspects of the electric vehicle being investigated. It captures the average state-space model of the converters utilized in the system, incorporating a comprehensive set of equations that account for the currents and voltages of each individual component. These equations are instrumental in defining the converters' behavior and their precise function in managing power flow within the system. By leveraging this well-defined mathematical model, researchers and engineers can thoroughly analyze and optimize the electric vehicle's performance under various operating conditions. This approach empowers them to enhance the vehicle's efficiency and effectiveness, ultimately contributing to the advancement of sustainable and eco-friendly transportation solutions. The use of a rigorously formulated model aids in developing smarter and more reliable electric vehicle systems, propelling the transition to greener and more environmentally friendly transportation alternatives.

$$\dot{x}_1 = \frac{V_{pv}}{L_p} - \frac{x_2}{L_p} + \frac{2x_2 u_{pv}}{L_p} + d \tag{3.2.1}$$

$$\dot{x}_2 = \frac{x_1}{C_p} - \frac{2x_2 u_{pv}}{C_p R_p} + \frac{x_2}{R_c} + d \tag{3.2.2}$$

$$\dot{x}_3 = \frac{V_{sc}}{L_{sc}} - \frac{x_4}{L_{sc}} + \frac{2x_4 u_{sc}}{L_{sc}} + d \tag{3.2.3}$$

$$\dot{x}_4 = \frac{x_3}{C_{sc}} - \frac{2x_4 u_{sc}}{C_{sc} R_{sc}} + \frac{x_4}{R_{sc}} + d \tag{3.2.4}$$

$$\dot{x}_5 = -\frac{R_g}{L_g} x_5 - \frac{(2u_1 - 1)}{L_g} x_6 + \frac{V_b}{L_g} + d \tag{3.2.5}$$

$$\dot{x}_6 = \frac{(2u_1 - 1)}{C_{dc}} x_5 - \frac{u_{23}}{C_{dc}} x_7 + d \tag{3.2.6}$$

$$\dot{x}_7 = -\frac{R_0}{L_d} x_5 - \frac{x_8}{L_d} + \frac{u_{23}}{L_d} x_6 + d \tag{3.2.7}$$

$$\dot{x}_8 = \frac{x_7}{C_d} - \frac{x_8}{C_d R_B} + \frac{x_9}{C_d R_B} + d \tag{3.2.8}$$

$$\dot{x}_9 = \frac{x_8}{C_{Bat} R_B} - \frac{x_9}{C_{Bat} R_B} + \frac{x_9}{C_{Bat} R_P} + d \tag{3.2.9}$$

The PV system's state-space model is represented by $\dot{x}_1$ and $\dot{x}_2$, while $\dot{x}_3$ and $\dot{x}_4$ correspond to the state-space model for the supercapacitor (SC). Additionally, the battery's state-space model is described by $\dot{x}_5$, $\dot{x}_6$, $\dot{x}_7$, $\dot{x}_8$, and $\dot{x}_9$. These equations capture crucial parameters, including the average grid current ($i$), the output voltage of the rectifier

(VDC), the inductor current (iL), the average output voltage of the DC-DC converter across capacitor Cd (VBat), and the average voltage across the battery capacitor (VC-bat).

Furthermore, the system accounts for external influences through a bounded disturbance $d(t)$. The disturbance is introduced to consider potential external factors affecting the system's performance. The bounds of this disturbance are specified as follows:

$$\delta_1 \leq d(t) \leq \delta_2 \qquad\qquad (3.2.10)$$

where $\delta_1$ and $\delta_2$ are the disturbance's lower and upper limits, respectively. Physically, the disturbance can be observed as switching spikes in the converter or any transient significant enough to test the proposed controllers.

## 3.3 Energy Management Strategy

An energy management system (EMS) is a system or framework designed to monitor, control, and optimize the energy consumption and usage of various devices, equipment, or systems within a building, facility, or organization [9].

## 3.4 Energy Management System for Photovoltaic Integration with Supercapacitor and Battery

This section presents an advanced Energy Management System (EMS) designed to optimize the integration of photovoltaic (PV) cells with energy storage devices, namely a supercapacitor bank and batteries as shown in Figure 3.2.

### 3.4.1 Energy Management System Architecture:

The proposed EMS consists of a PV array, a DC bus, a supercapacitor bank, a battery storage system, and a control unit. The PV array converts sunlight into electrical energy, which is then supplied to the DC bus. The control unit monitors the power flow and manages the energy distribution based on real-time power requirements. The EMS utilizes a hierarchical approach for energy utilization and storage [10]. The main

objective is to optimize the utilization of PV-generated power. When the PV production exceeds the immediate demand, the surplus power is directed towards charging the supercapacitor bank. Supercapacitors are chosen for their high power density and quick charge/discharge capabilities, making them well-suited for capturing and storing short-term excess power. In cases where the PV production exceeds both immediate demand and the supercapacitor storage capacity, the Energy Management System (EMS) automatically redirects the surplus energy towards charging the battery storage system. This efficient allocation of surplus energy ensures that renewable power sources are maximized, enhancing the overall performance and sustainability of the system. The EMS intelligently manages power distribution, ensuring optimal utilization of available resources and minimizing energy wastage, which is a significant step towards achieving more eco-friendly and energy-efficient solutions.

Batteries provide a higher energy density and longer discharge duration, enabling the storage of excess energy for extended periods.

## 3.4.2   Energy Deficit Management

During periods of insufficient PV generation, the EMS ensures uninterrupted power supply by drawing power from the battery and supercapacitor in a sequential manner. This sequential discharge strategy optimizes the use of stored energy and extends the system's autonomy during low or no PV production. The EMS control unit continuously monitors the PV generation, load demand, and energy storage levels. It employs intelligent algorithms to dynamically adjust the energy flow and prioritize the utilization of available resources. Real-time monitoring enables accurate system operation and efficient energy management [10].
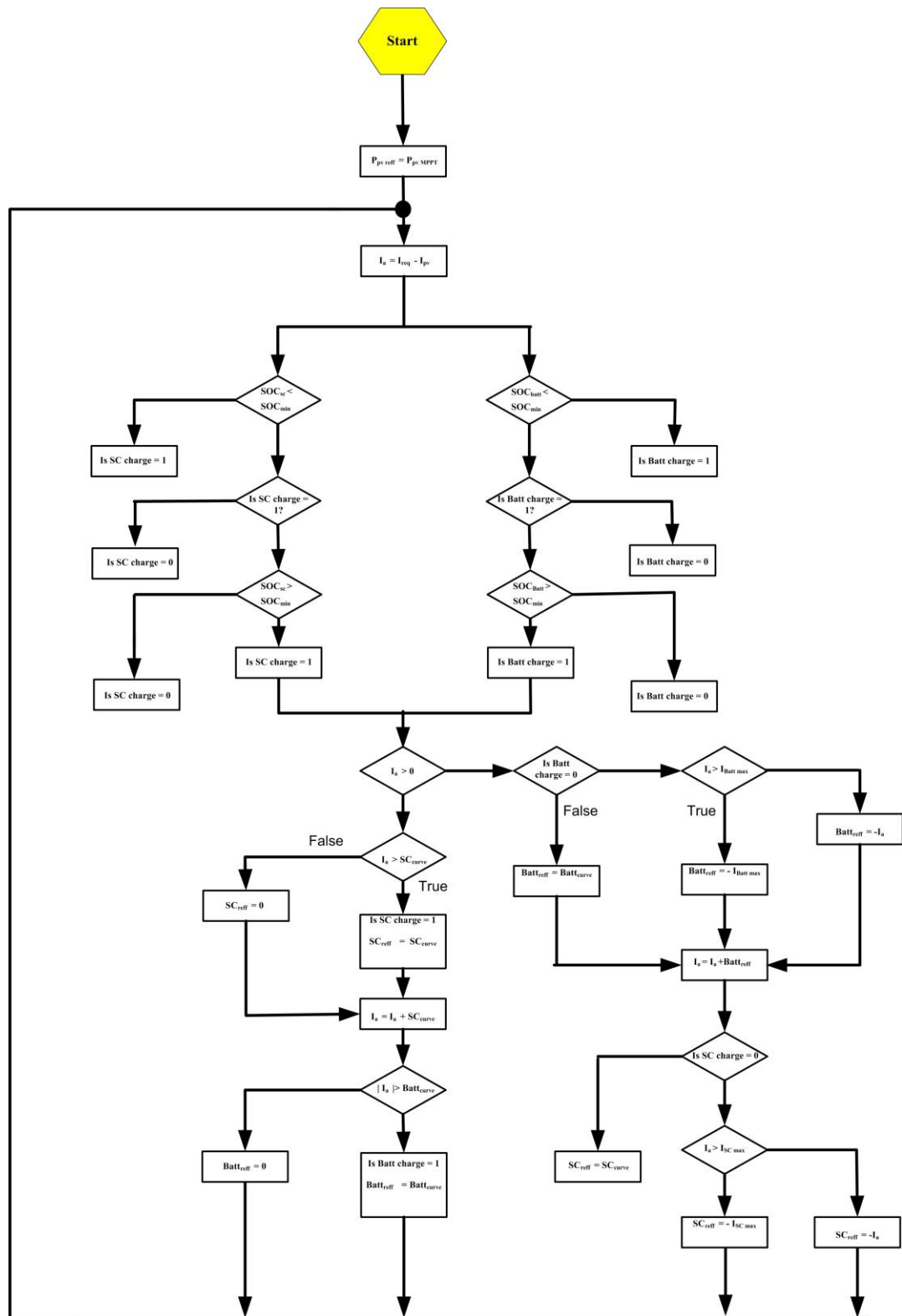
**Figure 3.2:** Energy Management System

# DESIGN OF NONLINEAR CONTROLLERS

## 4.1 Controller Design Objectives

In this section, we present the design of two controllers, namely the ITSMC and the STSMC, integrated within an energy management system, as depicted in Figure 4.1. The primary objective of these controllers is to address the challenges encountered during the control of DC-DC power converters. STSMC-based controllers for PV energy systems with energy storage result in reduced sensitivity to external variations and disturbances.

Moreover, our proposal introduces an energy management system that utilizes the STSMC approach to effectively distribute load demands between RESs and the ESS. The designed framework aims to achieve the following objectives:

1. MPPT of PV energy systems, ensuring optimal utilization of RESs by harnessing the maximum power available.

2. Accurate tracking of the battery's state currents to achieve their reference values, thereby reducing the system's reliance on RESs and enhancing overall efficiency.

3. Ensuring the global asymptotic stability of the entire system, guaranteeing a robust and reliable operation of the integrated PV and ESS setup.
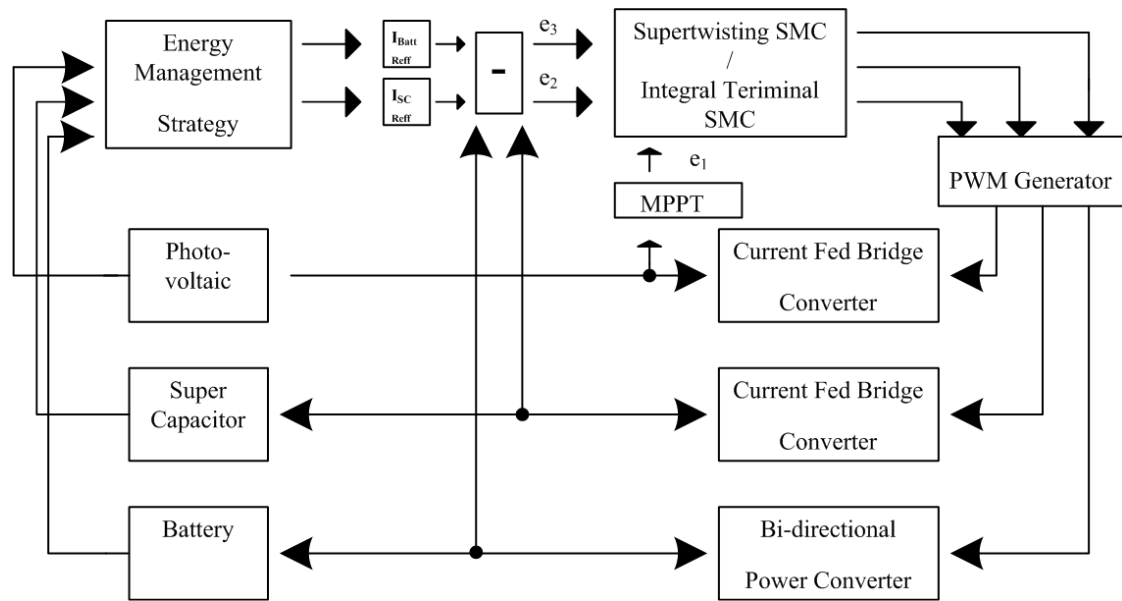
**Figure 4.1:** Energy Management System

**Table 4.1:** Parametric values of the controllers

| Controller | Parameters | Values |
|---|---|---|
| | C | $250 \times 10^{-3}$ |
| | L | $39 \times 10^{-3}$ |
| | R | 0.9 |
| | r | 0.4 |
| | kp | 5500 |
| | kw | 5000 |
| | ks | 3000 |
| | k1 | 2000 |
| | k2 | 1000 |
| | a1 | 2000 |
| | a2 | 1000 |
| | a3 | 4000 |

### 4.1.1 Integral Terminal Sliding Mode Controller (ITSMC) Design for PV and SC Energy System

ITSMC is a variant of sliding mode control that incorporates integral terms of errors to reduce steady-state errors [11]. In the context of the PV and SC systems, a PV module serves to convert solar energy into electricity. By combining multiple PV modules, we create a PV array, allowing for increased power generation capacity from the solar energy harvested. The efficiency of the PV array depends on environmental factors such as irradiance and temperature. To maximize power output from the PV array, the duty cycle of the DC-DC current converter is adjusted by varying it. This adjustment is achieved using a neural network-based MPPT algorithm [12], which provides more precise results and requires less time compared to conventional perturb and observe-based MPPT algorithms. The neural network is optimized to determine the MPPV reference at which the PV array should operate due to the intermittent nature of solar energy.

Conversely, a supercapacitor, also referred to as an ultracapacitor, serves as an energy storage device with an exceptional ability to rapidly store and release substantial amounts of electrical energy. Differing from traditional batteries, supercapacitors store energy within an electrostatic field rather than through chemical reactions. One of their primary advantages lies in their remarkable power density, enabling them to efficiently store and discharge energy at a significantly faster rate compared to conventional batteries. As a result, supercapacitors find practical applications in scenarios where high power output is essential for short bursts of energy. They are particularly useful in electric vehicles, providing quick bursts of power for acceleration. Additionally, supercapacitors have a long cycle life, enabling them to be charged and discharged numerous times without significant degradation in performance, unlike traditional batteries that tend to degrade over time and require replacement. Moreover, supercapacitors can operate over a wide range of temperatures, making them suitable for use in extreme environments.

To achieve maximum power generation from the RES, we track the PV array and SC current state ($\dot{x}_1$ and $\dot{x}_3$) to their desired values ($\dot{x}_{1reff}$ and $\dot{x}_{3reff}$) using an error term in the energy system controller.

$$e_1 = x_1 - x_{1reff} \tag{4.1.1}$$

$$e_3 = x_3 - x_{3reff} \qquad (4.1.2)$$

Time derivative of the above mentioned error is equal to:

$$\dot{e}_1 = \dot{x}_1 - \dot{x}_{1reff} \qquad (4.1.3)$$

$$\dot{e}_3 = \dot{x}_3 - \dot{x}_{3reff} \qquad (4.1.4)$$

Putting value of $\dot{x}_1$ and $\dot{x}_3$ we get;

$$\dot{e}_1 = \frac{V_{pv}}{L_p} - \frac{x_2}{L_p} + \frac{2x_2 u_{pv}}{L_p} + d - \dot{x}_{1reff} \qquad (4.1.5)$$

$$\dot{e}_3 = \frac{V_{sc}}{L_{sc}} - \frac{x_4}{L_{sc}} + \frac{2x_4 u_{sc}}{L_{sc}} + d - \dot{x}_{3reff} \qquad (4.1.6)$$

Since both the state space models of the PV and SC energy systems have a single control input, a common sliding surface has been chosen for both systems as follows:

$$S_1 = e_1 + \lambda \left( \int e_1 dt \right)^{\frac{p}{q}} \qquad (4.1.7)$$

$$S_2 = e_3 + \lambda \left( \int e_3 dt \right)^{\frac{p}{q}} \qquad (4.1.8)$$

Time derivative of the above sliding surface is:

$$\dot{S}_1 = \dot{e}_1 + e_1 \lambda \frac{p}{q} \left( \int e_1 dt \right)^{\frac{p}{q} - 1} \qquad (4.1.9)$$

$$\dot{S}_2 = \dot{e}_3 + e_3 \lambda \frac{p}{q} \left( \int e_3 dt \right)^{\frac{p}{q} - 1} \qquad (4.1.10)$$

For $u_{eq1}$ put $\dot{S}_1 = 0$ and for $u_{eq2}$ put $\dot{S}_2 = 0$;

$$\dot{S}_1 = \frac{V_{pv}}{L_p} - \frac{x_2}{L_p} + \frac{2x_2 u_{pv}}{L_p} + d - \dot{x}_{1reff} + e_1 \lambda \frac{p}{q} \left( \int e_1 dt \right)^{\frac{p}{q} - 1} \qquad (4.1.11)$$

$$\dot{S}_2 = \frac{V_{sc}}{L_{sc}} - \frac{x_4}{L_{sc}} + \frac{2x_4 u_{sc}}{L_{sc}} + d - \dot{x}_{3reff} + e_3 \lambda \frac{p}{q} \left( \int e_3 dt \right)^{\frac{p}{q} - 1} \qquad (4.1.12)$$

To prove the stability of the system, Lyapunov candidate function is taken as:

17

$$V = \frac{S_1^2}{2} + \frac{S_2^2}{2} \tag{4.1.13}$$

$$\dot{V} = S_1\dot{S_1} + S_2\dot{S_2} \tag{4.1.14}$$

$$\dot{V} = S_1\left(\dot{e}_1 + e_1\lambda(p/q)\left(\int e_1 dt\right)^{p/q-1}\right) + S_2\left(\dot{e}_3 + e_3\lambda(p/q)\left(\int e_3 dt\right)^{p/q-1}\right) \tag{4.1.15}$$

$$\dot{V} = S_1\left(\frac{V_{pv}}{L_p} - \frac{x_2}{L_p} + \frac{2x_2u_{pv}}{L_p} + d - \dot{x}_{1reff} + e_1\lambda(p/q)\left(\int e_1 dt\right)^{p/q-1}\right)$$
$$+ S_2\frac{V_{sc}}{L_{sc}} - \frac{x_4}{L_{sc}} + \frac{2x_4u_{sc}}{L_{sc}} + d - \dot{x}_{3reff} + {}_3\lambda(p/q)\left(\int e_3 dt\right)^{p/q-1} \tag{4.1.16}$$

To make V negative definite, let us take:

$$-k_{pv}sign(S_1) = \frac{V_{pv}}{L_p} - \frac{x_2}{L_p} + \frac{2x_2u_{pv}}{L_p} + d - \dot{x}_{1reff} + e_1\lambda(p/q)\left(\int e_1 dt\right)^{p/q-1} \tag{4.1.17}$$

$$-k_{sc}sign(S_2) = \frac{V_{sc}}{L_{sc}} - \frac{x_4}{L_{sc}} + \frac{2x_4u_{sc}}{L_{sc}} + d - \dot{x}_{3reff} + e_3\lambda(p/q)\left(\int e_3 dt\right)^{p/q-1} \tag{4.1.18}$$

Solving Eqs. for control inputs $u_{pv}$ and $u_{sc}$ following control laws are obtained:

$$u_{pv} = \frac{1}{2} - \frac{V_{pv}}{2x_2} - \frac{L_p}{2x_2}\left(e_1\lambda(p/q)\left(\int e_1 dt\right)^{p/q-1} + \dot{x}_{1ref} - d\right) - k_{pv}sign(S_1) \tag{4.1.19}$$

$$u_{sc} = \frac{1}{2} - \frac{V_{sc}}{2x_4} - \frac{L_{sc}}{2x_6}\left(e_3\lambda(p/q)\left(\int e_3 dt\right)^{p/q-1} + \dot{x}_{3ref} - d\right) - k_{sc}sign(S_2) \tag{4.1.20}$$

Putting the values from Eqs. $\dot{V}$ can be calculated as:

$$\dot{V} = -k_{pv}S_1sign(S_1) - k_{sc}S_2sign(S_2) \tag{4.1.21}$$

which shows that system is asymptotically stable and all errors will converge to zero in finite time.

## 4.1.2 Integral Terminal Sliding Mode Controller (ITSMC) Design for Battery

During G2V mode, the converter acts as a boost rectifier, facilitating a two-stage CC-CV charge to efficiently recharge the EV battery. In V2G mode, it functions as an inverter, conducting a single CC operation with a negative current reference to efficiently discharge the battery and supply power to the grid. To achieve the desired CC-CV operation, a DC-DC converter is employed, and the controller must effectively manage the switching dynamics of both the DC-DC and AC-DC converters to ensure stable and efficient converter operation. Additionally, the controller needs to handle uncertainties and nonlinearities in the system, such as variations in load conditions, input voltage, and frequency changes, to ensure safe and reliable converter operation.

Battery controller objectives:

1. Achieve maximum power factor (MPF) for grid current and voltage synchronization.

2. Regulate DC bus voltage to desired levels.

3. Enable CC-CV operation in G2V mode and CC operation in V2G mode.

4. Ensure safe battery charging and discharging [13].

In order to accurately track the average grid current ($i$) and inductor current ($i_L$) to their desired state values ($\dot{x}_{5reff}$ and $\dot{x}_{7reff}$) for achieving maximum power generation, we define the error term for designing the battery controller as follows:

$$e_5 = x_5 - x_{5reff} \tag{4.1.22}$$

$$e_7 = x_7 - x_{7reff} \tag{4.1.23}$$

Time derivative of the above mentioned error is equal to:

$$\dot{e}_5 = \dot{x}_5 - \dot{x}_{5reff} \tag{4.1.24}$$

$$\dot{e}_7 = \dot{x}_7 - \dot{x}_{7reff} \tag{4.1.25}$$

Putting value of $\dot{x}_5$ and $\dot{x}_7$ we get;

$$\dot{e}_5 = -\frac{R_g}{L_g}x_5 - \frac{(2u_1 - 1)x_6}{L_g} + \frac{V_b}{L_g} + d - \dot{x}_{5reff} \tag{4.1.26}$$

$$\dot{e}_7 = -\frac{R_0}{L_d}x_5 - \frac{x_8}{L_d} + \frac{u_{23}}{L_d}x_6 + d - \dot{x}_{7reff} \tag{4.1.27}$$

As the state space model of battery system have two control input, so there will be two sliding surface which is:

$$S_3 = e_5 + \lambda \left( \int e_5 dt \right)^{\frac{p}{q}} \tag{4.1.28}$$

$$S_4 = e_7 + \lambda \left( \int e_7 dt \right)^{\frac{p}{q}} \tag{4.1.29}$$

Time derivative of the above sliding surface is:

$$\dot{S_3} = \dot{e}_5 + e_5 \lambda \frac{p}{q} \left( \int e_5 dt \right)^{\frac{p}{q}-1} \tag{4.1.30}$$

$$\dot{S_4} = \dot{e}_7 + e_7 \lambda \frac{p}{q} \left( \int e_7 dt \right)^{\frac{p}{q}-1} \tag{4.1.31}$$

For $u_{eq3}$ put $\dot{S_3} = 0$ and for $u_{eq4}$ put $\dot{S_4} = 0$;

$$\dot{S_3} = -\frac{R_g}{L_g} x_5 - \frac{(2u_1 - 1)x_6}{L_g} + \frac{V_b}{L_g} + d - \dot{x}_{5reff} + e_5\lambda(p/q) \left( \int e_5 dt \right)^{p/q-1} \tag{4.1.32}$$

$$\dot{S_4} = -\frac{R_0}{L_d} x_5 - \frac{x_8}{L_d} + \frac{u_{23}}{L_d} x_6 + d - \dot{x}_{7reff} + e_7\lambda(p/q \left( \int e_7 dt \right)^{p/q-1} \tag{4.1.33}$$

To prove the stability of the system, Lyapunov candidate function is taken as:

$$V = \frac{S_3^2}{2} + \frac{S_4^2}{2} \tag{4.1.34}$$

$$\dot{V} = S_3 \dot{S_3} + S_4 \dot{S_4} \tag{4.1.35}$$

$$\dot{V} = S_3 \left( \dot{e}_5 + e_5\lambda(p/q) \left( \int e_5 dt \right)^{p/q-1} \right) + S_4 \left( \dot{e}_7 + e_7\lambda(p/q) \left( \int e_7 dt \right)^{p/q-1} \right) \tag{4.1.36}$$

$$\dot{V} = S_3 \left( -\frac{R_g}{L_g} x_5 - \frac{(2u_1 - 1)x_6}{L_g} + \frac{V_b}{L_g} + d - \dot{x}_{5reff} + e_5\lambda(p/q) \left( \int e_5 dt \right)^{p/q-1} \right)$$

$$+ S_4 \left( \frac{R_0}{L_d} x_5 - \frac{x_8}{L_d} + \frac{u_{23}}{L_d} x_6 + d - \dot{x}_{7reff} + e_7\lambda(p/q) \left( \int e_7 dt \right)^{p/q-1} \right) \tag{4.1.37}$$

To make V negative definite, let us take:

$$-k_1 sign\,(S_3) =$$

$$S_3 \left( -\frac{R_g}{L_g} x_5 - \frac{(2u_1 - 1)}{Lg} x_6 + \frac{V_b}{Lg} + d - x_{5reff} + e_5\lambda(p/q) \left( \int e_5 dt \right)^{p/q-1} \right) \tag{4.1.38}$$

$$-k_2 sign\left(S_4\right) =$$

$$S_4 \quad -\frac{R_0}{L_d}x_5 \quad -\frac{x_8}{L_d} \quad +\frac{u_{23}}{L_d}x_6 + d - \dot{x}_{7reff} + e_7\lambda(p/q) \quad \int e_7 dt \quad {}^{p/q-1} \quad !$$

$$(4.1.39)$$

Solving Eqs. for control inputs $u_1$ and $u_{23}$ following control laws are obtained:

$$u_1 = -\frac{L_g}{2x_6}\left(\frac{Rx_5}{L_g} + \frac{V_b}{L_g} + \frac{x_6}{L_g} + \dot{x}_{5ref} - d\right) + (e_5\lambda(p/q))\int e_5 dt^{p/q-1} - k_1 sign\left(S_3\right)$$

$$(4.1.40)$$

$$u_{23} = -\frac{L_d}{x_6}\left(\frac{Rx_5}{L_d} + \frac{x_8}{L_d} + \dot{x}_{7ref} - d\right) + (e_7\lambda(p/q))\int e_7 dt^{p/q-1} - k_2 sign\left(S_4\right)$$

$$(4.1.41)$$

Putting the values from Eqs. can be calculated as:

$$\dot{V} = -k_1 S_3 sign\left(S_3\right) - k_2 S_4 sign\left(S_4\right)$$

which shows that system is asymptotically stable and all errors will converge to zero in finite time.

### 4.1.3 Super Twisting Sliding Mode Controller (STSMC) Design for PV and SC Energy System

The STSMC is a powerful SMC technique widely employed in various control systems [13]. Introduced by Levant in 1993, STSMC extends traditional sliding mode control to achieve enhanced performance and robustness.

Key characteristics of the Super Twisting Sliding Mode Controller:

1. Robustness: STSMC effectively handles system uncertainties, disturbances, and parameter variations by driving the system dynamics to adhere to a predetermined sliding surface. This feature ensures robust performance even in the presence of external perturbations.

2. Finite-time convergence: STSMC guarantees that the system state converges to the sliding surface within a finite time, enabling control objectives to be achieved promptly and reliably.

3. Chattering suppression: Traditional sliding mode control can exhibit chattering, characterized by high-frequency switching of the control signal. STSMC overcomes this

issue by incorporating a continuous reaching law that minimizes chattering, leading to smoother and more stable control actions.

4. Nonlinear control action: STSMC's control action is inherently nonlinear due to the presence of the saturation function and the sign function. The saturation function restricts the control input within a specified range, while the sign function extracts the sign of the sliding surface, contributing to the controller's robustness.

5. Gain tuning: The performance of STSMC is influenced by the careful selection of the control gain parameter [14]. Proper tuning of this gain is crucial to achieving the desired control performance and stability.

STSMC finds applications in diverse control systems, including robotics, power electronics, aerospace systems, and mechanical systems. It excels in systems with uncertainties and disturbances that demand robust and rapid control responses.

The primary objective of STSMC is to furnish robust and precise control for dynamic systems, especially those exhibiting high levels of nonlinearities, using a sliding surface that incorporates a second-order sliding mode term for faster convergence and improved tracking performance.

To design the PV and SC energy system controller, we define the error term as follows:

$$e_1 = x_1 - x_{1reff} \tag{4.1.43}$$

$$e_3 = x_3 - x_{3reff} \tag{4.1.44}$$

Time derivative of the above mentioned error is equal to:

$$\dot{e}_1 = \dot{x}_1 - \dot{x}_{1reff} \tag{4.1.45}$$

$$\dot{e}_3 = \dot{x}_3 - \dot{x}_{3reff} \tag{4.1.46}$$

Putting value of $\dot{x}_1$ and $\dot{x}_3$ we get;

$$\dot{e}_1 = \frac{V_{pv}}{L_p} - \frac{x_2}{L_p} + \frac{2x_2 u_{pv}}{L_p} + d - \dot{x}_{1reff} \tag{4.1.47}$$

$$\dot{e}_3 = \frac{V_{sc}}{L_{sc}} - \frac{x_4}{L_{sc}} + \frac{2x_4 u_{sc}}{L_{sc}} + d - \dot{x}_{3reff} \tag{4.1.48}$$

As the state space model of PV and SC energy system respectively both have single control input, so for both there will be one sliding surface has been selected as follows:

$$S_1 = a_1.e_1 \tag{4.1.49}$$

$$S_2 = a_3.e_3 \tag{4.1.50}$$

Time derivative of the above sliding surface is:

$$\dot{S}_1 = a_1.\dot{e}_1 \tag{4.1.51}$$

$$\dot{S}_3 = a_3.\dot{e}_3 \tag{4.1.52}$$

Putting value of $\dot{x}_1$ and $\dot{x}_3$ we get;

$$\dot{S}_1 = a_1. \left( \frac{V_{pv}}{L_p} - \frac{x_2}{L_p} + \frac{2x_2 u_{pv}}{L_p} + d - \dot{x}_{1reff} \right) \tag{4.1.53}$$

$$\dot{S}_2 = a_2. \left( \frac{V_{sc}}{L_{sc}} - \frac{x_4}{L_{sc}} + \frac{2x_4 u_{sc}}{L_{sc}} + d - \dot{x}_{3reff} \right) \tag{4.1.54}$$

For analyzing the stability, we consider the following Lyapunov candidate function as:

$$V = \frac{S^2_1}{2} + \frac{S^2_2}{2} \tag{4.1.55}$$

$$\dot{V} = S_1 \dot{S}_1 + S_2 \dot{S}_2 \tag{4.1.56}$$

$$\dot{V} = S_1 \left( a_1. \left( \frac{V_{pv}}{L_p} - \frac{x_2}{L_p} + \frac{2x_2 u_{pv}}{L_p} + d - \dot{x}_{1reff} \right) \right)$$
$$+ S_2 \left( a_2. \left( \frac{V_{sc}}{L_{sc}} - \frac{x_4}{L_{sc}} + \frac{2x_4 u_{sc}}{L_{sc}} + d - \dot{x}_{3reff} \right) \right) \tag{4.1.57}$$

In order to make the derivative of Lyapunov function negative definite, we have to impose the following constraint:

$$\dot{S1} = -\psi_{pv} /S_1/^\alpha \operatorname{sat}(S_1) - \psi_{pv} \int \operatorname{sat}(S_1) \, dt \tag{4.1.58}$$

$$\dot{S2} = -\psi_{sc} /S_2/^\beta \operatorname{sat}(S_2) - \psi_{sc} \int \operatorname{sat}(S_2) \, dt \tag{4.1.59}$$

Now plugging the value of $\dot{S}_1$ and $\dot{S}_2$

$$a_1. \frac{V_{pv}}{L_p} - \frac{x_2}{L_p} + \frac{2x_2 u_{pv}}{L_p} + d - \dot{x}_{1ref} = -\psi_{pv} /S_1/^\alpha \operatorname{sat}(S_1) - \psi_{pv} \int \operatorname{sat}(S_1) \, dt \tag{4.1.60}$$

$$a_2. \frac{V_{sc}}{L_{sc}} - \frac{x_4}{L_{sc}} + \frac{2x_4 u_{sc}}{L_{sc}} + d - \dot{x}_{3ref} = -\psi_{sc} /S_2/^\beta \operatorname{sat}(S_2) - \psi_{sc} \int \operatorname{sat}(S_2) \, dt \tag{4.1.61}$$

Now the overall controller $u_{(pv)STSMC}$ and $u_{(sc)STSMC}$ can be obtained as:

$$u_{(pv)STSMC} = \frac{L_p}{2a_1x_2}\left[-a_1\frac{V_{pv}}{L_p} + a_1\frac{x_2}{L_p} - a_1d + a_1\dot{x}_{1_{reff}}\right] + \frac{L_p}{2a_1x_2}\left[\psi_{pv}/S_1/^\alpha \operatorname{sat}(S_1) + \psi_{pv}\int \operatorname{sat}(S_1)\,dt\right]$$

(4.1.62)

$$u_{(sc)STSMC} = \frac{L_p}{2a_1x_2}\left[-a_2\frac{V_{sc}}{L_{sc}} + a_2\frac{x_4}{L_p} - a_2d + a_2\dot{x}_{3_{reff}}\right] + \frac{L_p}{2a_1x_2}\left[\psi_{sc}/S_2/^\beta \operatorname{sat}(S_2) + \psi_{sc}\int \operatorname{sat}(S_2)\,dt\right]$$

(4.1.63)

Now Eq. (4.1.62) and Eq. (4.1.63) can be simplified as:

$$\dot{V} = -S_1\left[\psi_{pv}/S_1/^\alpha \operatorname{sat}(S_1) - \psi_{pv}\int \operatorname{sat}(S_1)\,dt\right] - S_2\left[\psi_{sc}/S_2/^\beta \operatorname{sat}(S_2) - \psi_{sc}\int \operatorname{sat}(S_2)\,dt\right]$$

(4.1.64)

which shows that system is asymptotically stable and all errors will converge to zero in finite time.

### 4.1.4 Super twisting sliding controller (STSMC) design for for battery system.

We define error terms for designing of the battery system controller as follows:

$$e_5 = x_5 - x_{5reff} \tag{4.1.65}$$

$$e_7 = x_7 - x_{7reff} \tag{4.1.66}$$

Time derivative of the above mentioned error is equal to:

$$\dot{e}_5 = \dot{x}_5 - \dot{x}_{5reff} \tag{4.1.67}$$

$$\dot{e}_7 = \dot{x}_7 - \dot{x}_{7reff} \tag{4.1.68}$$

Putting value of $\dot{x}_5$ and $\dot{x}_7$ we get:

$$\dot{e}_5 = -\frac{R_g}{L_g}x_5 - \frac{(2u_1 - 1)}{L_g}x_6 + \frac{V_b}{L_g} + d - \dot{x}_{5_{reff}} \tag{4.1.69}$$

$$\dot{e}_7 = -\frac{R_0}{L_d}x_5 - \frac{x_8}{L_d} + \frac{u_{23}}{L_d}x_6 + d - \dot{x}_{7_{reff}} \tag{4.1.70}$$

The state space model of battery system have two control input, so there will be two sliding surface which is:

$$S_3 = a_5.e_5 \tag{4.1.71}$$

$$S_4 = a_7.e_7 \tag{4.1.72}$$

Time derivative of the above sliding surface is:

$$\dot{S_3} = a_5.\dot{e_5} \tag{4.1.73}$$

$$\dot{S_4} = a_7.\dot{e_7} \tag{4.1.74}$$

Putting value of $\dot{x_5}$ and $\dot{x_7}$ we get:

$$\dot{S_3} = a_5 \left( -\frac{R_g}{L_g}x_5 - \frac{(2u_1 - 1)}{L_g}x_6 + \frac{V_b}{L_g} + d - \dot{x}_{5\,reff} \right) \tag{4.1.75}$$

$$\dot{S_4} = a_7 \left( -\frac{R_0}{L_d}x_5 - \frac{x_8}{L_d} + \frac{u_{23}}{L_d}x_6 + d - \dot{x}_{7\,reff} \right) \tag{4.1.76}$$

For analyzing the stability, we consider the following Lyapunov candidate function as:

$$V = \frac{S_3^2}{2} + \frac{S_4^2}{2} \tag{4.1.77}$$

$$\dot{V} = S_3\dot{S_3} + S_4\dot{S_4} \tag{4.1.78}$$

$$\dot{V} = S_3 \left( a_5 \left( -\frac{R_g}{L_g}x_5 - \frac{(2u_1 - 1)}{L_g}x_6 + \frac{V_b}{L_g} + d - \dot{x}_{5reff} \right) \right)$$

$$+ S_4 \left( a_7 \left( -\frac{R_0}{L_d}x_5 - \frac{x_8}{Ld} + \frac{u_{23}}{L_d}x_6 + d - \dot{x}_{7\,reff} \right) \right) \tag{4.1.79}$$

To make the derivative of Lyapunov function negative definite, we have to impose the following constraint:

$$\dot{S_3} = -\psi_3 \,|S|^\gamma \, sat\,(S_3) - \psi_3 \int sat\,(S_3)\,dt \tag{4.1.80}$$

$$\dot{S_4} = -\psi_4 \,|S|^\delta \, sat\,(S_4) - \psi_4 \int sat\,(S_4)\,dt \tag{4.1.81}$$

Now plugging the value of $\dot{S_3}$ and $\dot{S_4}$:

$$a_5 \left( -\frac{R_g}{L_g}x_5 - \frac{(2u_1 - 1)}{L_g}x_6 + \frac{V_b}{L_g} + d - \dot{x}_{5_{reff}} \right) = -\psi_3 \,|S|^\gamma \, sat\,(S_3) - \psi_3 \int sat\,(S_3)\,dt$$

$$\tag{4.1.82}$$

$$a_7 \left( -\frac{R_0}{L_d}x_5 - \frac{x_8}{L_d} + \frac{u_{23}}{L_d}x_6 + d - \dot{x}_{7_{reff}} \right) = -\psi_4 \,|S|^\delta \, sat\,(S_4) - \psi_4 \int sat\,(S_4)\,dt$$

$$\tag{4.1.83}$$

Now the overall controller $u_{(1)STSMC}$ and $u_{(23)STSMC}$ can be obtained as:

$$u_{(1)STSMC} =$$
$$\frac{L_g}{2x_6} \left( -a_5x_5\frac{R_g}{L_g} + a_5\frac{x_6}{L_g} + a_5\frac{V_b}{L_g} + a_5d + a_5\dot{x}_{5_{reff}} \right) + \frac{L_g}{2x_6} \left( -\psi_3\,|S|^\gamma\, sat\,(S_3) - \psi_3 \int sat\,(S_3)\,dt \right)$$

$$\tag{4.1.84}$$

$$u_{(23)STSMC} =$$

$$\frac{L_d}{x_6}\left[-a_7 x_5 \frac{R_0}{L_d} + a_7 \frac{x_8}{L_d} + a_7 \frac{\dot{x}_d}{L_d} + a_7 d + a_7 \dot{x}_{7_{reff}}\right] + \frac{L_d}{x_6}\left[-\psi_4 |S|^\delta sat(S_4) - \psi_4 \int sat(S_4) dt\right]$$

$$(4.1.85)$$

Now Eq. (4.1.84) and Eq. (4.1.85) can be simplified as:

$$\dot{V} = -S_3\left[\psi_3 |S_3|^\alpha sat(S_3) - \psi_3 \int sat(S_3) dt\right] - S_4\left[\psi_4 |S_4|^\beta sat(S_4) - \psi_4 \int sat(S_4) dt\right]$$

$$(4.1.86)$$

which shows that system is asymptotically stable and all errors will converge to zero in finite time.
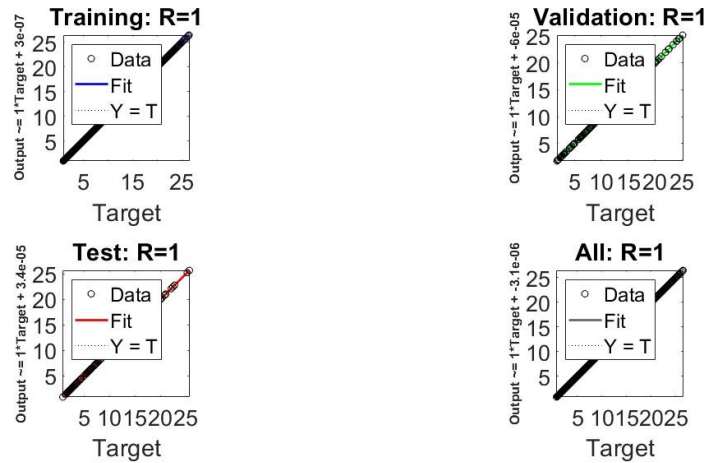
**Figure 4.2:** Regression plot.

## 4.2 Design of ANN-based Maximum Power Point Tracking (MPPT)

A PV module serves as a clean and pollution-free means of converting solar energy into electricity, and when multiple modules are combined, they form a PV array. The efficiency of this PV array depends on environmental factors such as irradiance and temperature. To ensure maximum power output from the PV array, the duty cycle of the DC-DC current converter is adjusted by varying it accordingly. This adjustment is accomplished through a neural network-based Maximum Power Point Tracking (MPPT) algorithm [15]. Compared to conventional perturb and observe-based MPPT algorithms, the neural network-based approach provides more precise results and operates with reduced computational time.

The neural network used in the MPPT algorithm has been optimized to determine the reference voltage for the MPPV at which the PV array should operate. This optimization accounts for the intermittent nature of solar energy and ensures that the PV system efficiently harnesses available solar power throughout varying environmental conditions.

# Gray Wolf Optimization

The Gray Wolf Optimization algorithm is a nature-inspired metaheuristic optimization technique based on the social hierarchy and hunting behavior of gray wolves [16]. Proposed by Mirjalili et al. in 2014, this algorithm has demonstrated its efficacy in addressing various optimization problems in engineering, economics, and other domains.

## 5.1 Controller Tuning through Optimization

The algorithm emulates the social hierarchy and hunting behavior of a pack of gray wolves. In this approach, each wolf represents a potential solution to the optimization problem, and its fitness is evaluated based on the objective function of the problem. Initially, the algorithm starts with a population of wolves randomly distributed across the search space. The wolves are ranked based on their fitness values, with the alpha wolf representing the best solution, followed by the beta, delta, and omega wolves.

Once the pack hierarchy is established, the wolves collaboratively search for optimal solutions within the search space. Each wolf updates its position based on its own experience and the collective experiences of other wolves in the pack. The update rules are as follows:

- Alpha wolf: The alpha wolf updates its position by moving towards a promising region in the search space, which is a weighted average of the positions of the beta, delta, and omega wolves.

- Beta wolf: The beta wolf updates its position by moving towards a promising

**Table 5.1:** Optimization Parameter

| Controller gain | Search limits | Gain value | Fitness function value |
|:---:|:---:|:---:|:---:|
| Kp1 | 1 to 500 | 273.74 | 52.24 |
| Kp2 | 1 to 100 | 19.84 | 52.24 |
| Ks1 | 1 to 100 | 12.03 | 531.8 |
| Ks2 | 1 to 500 | 279.98 | 531.8 |

region in the search space, which is a weighted average of the positions of the delta and omega wolves.

- Delta wolf: The delta wolf updates its position by moving towards a promising region in the search space, which is a weighted average of the positions of the alpha and beta wolves.

- Omega wolf: The omega wolf updates its position by moving randomly within the search space.

The algorithm iteratively continues until a stopping criterion is met, such as a maximum number of iterations or the attainment of a satisfactory solution. The best solution found by the algorithm corresponds to the position of the alpha wolf at the conclusion of the search process.

## 5.2  Optimization  Summary

The Gray Wolf Optimization algorithm is a potent optimization technique inspired by the behavior of gray wolves in nature. It has exhibited promising outcomes in tackling various optimization problems and is widely adopted in diverse fields for controller tuning and the discovery of optimal solutions.
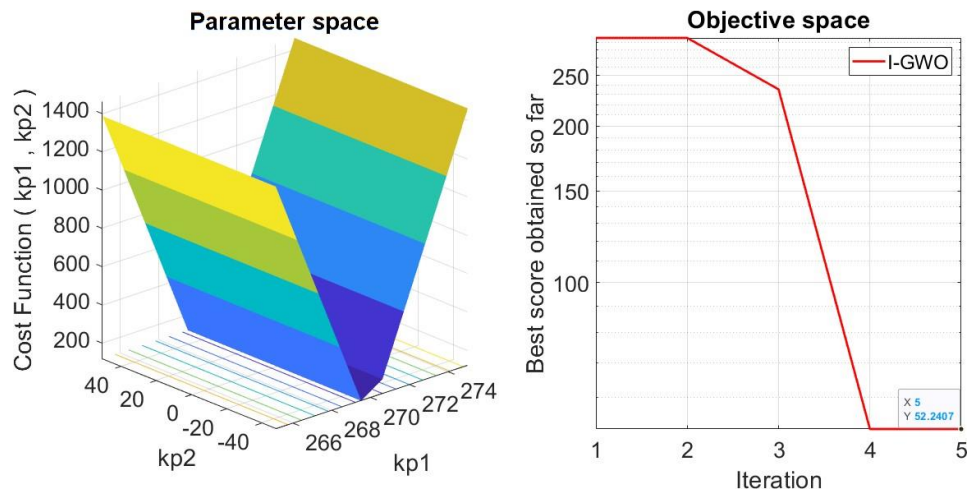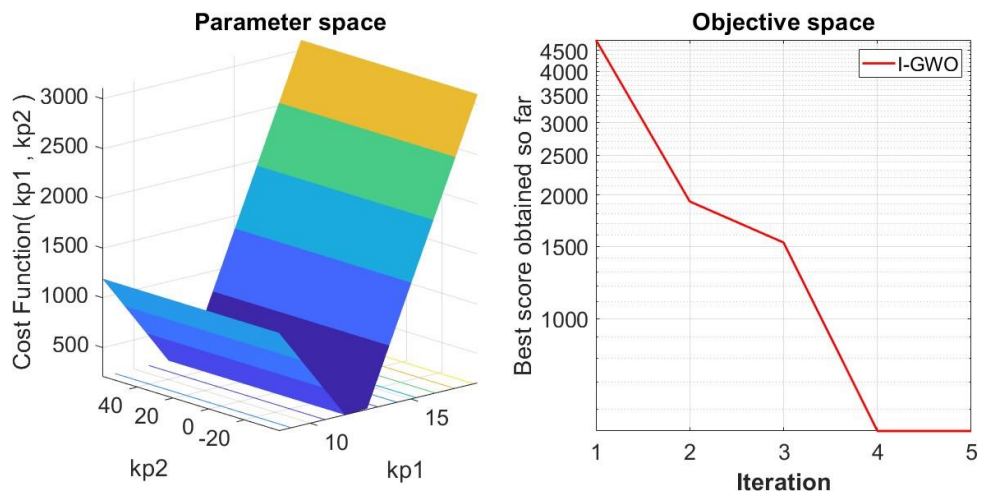
**Figure 5.1:** PV optimization results



**Figure 5.2:** SC optimization results

# Simulation Results

The proposed controller has been validated using the MATLAB/Simulink platform. Table 1 lists the optimization parameters, and Table 2 lists the controller parameters used in the simulations. The system is subjected to a disturbance, as shown in Figure **??**, to demonstrate the robustness of the proposed controllers.

### 6.0.1 PV Energy System Simulation Results

In this section, the performance of the proposed controllers (Eq. 29 and 71) is evaluated under the influence of state disturbances, as shown in Figure 6.1. The output current extracted from the PV panel using the Artificial Neural Network (ANN) is analyzed in Figure 6.2, which demonstrates that the chattering effect is significantly reduced by the STSMC compared to the ITSMC. Figure 6.3 presents the control input $u_{pv}$.
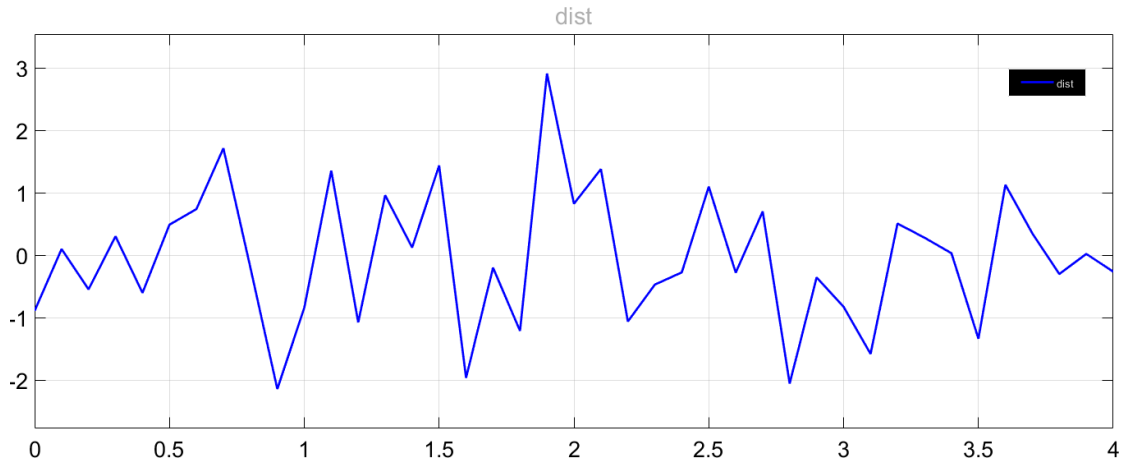
### 6.0.2 SC energy system simulation results

The proposed controller in Eq. (30 and 72) has been simulated in the same environment along with the comparison to verify the performance and tracking of SC current. Fig. 6.4 shows the SC current generated against the reference current while the Fig. 6.5. shows the control input $u_{sc}$.
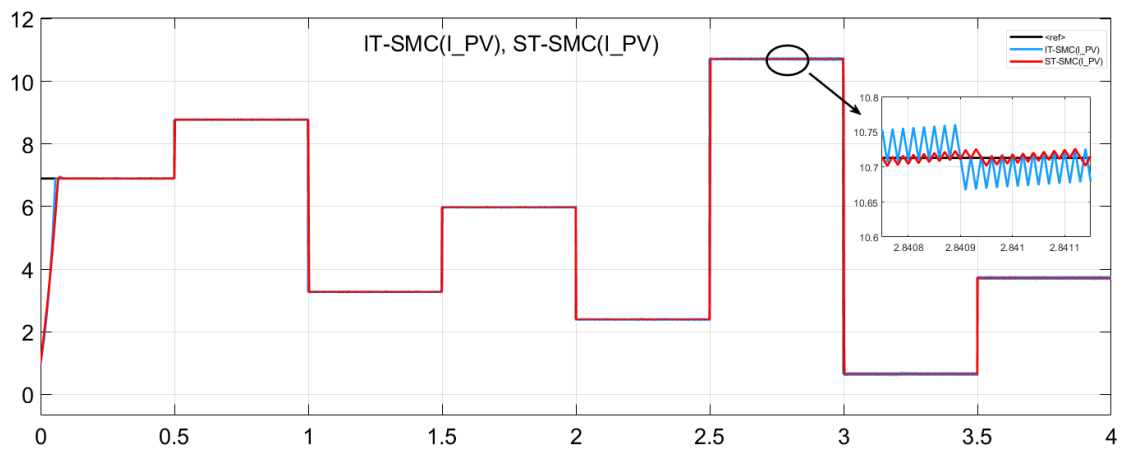
### 6.0.3 Battery energy system simulation results

The Fig.6.5 shows the grid current and and grid voltage which is derived in Eq. (50 and 94) along with the comparison of proposed controllers.
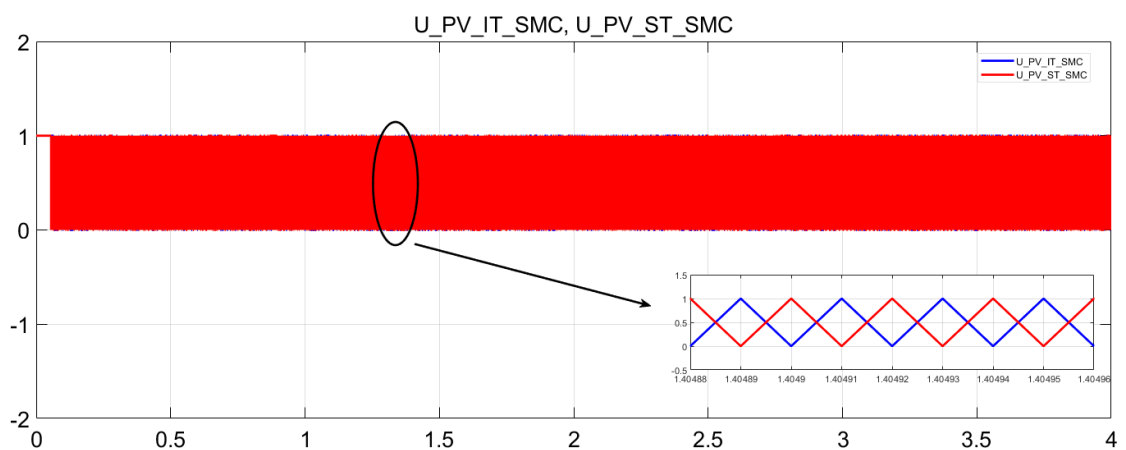
**Figure 6.1:** State Disturbance d(t)
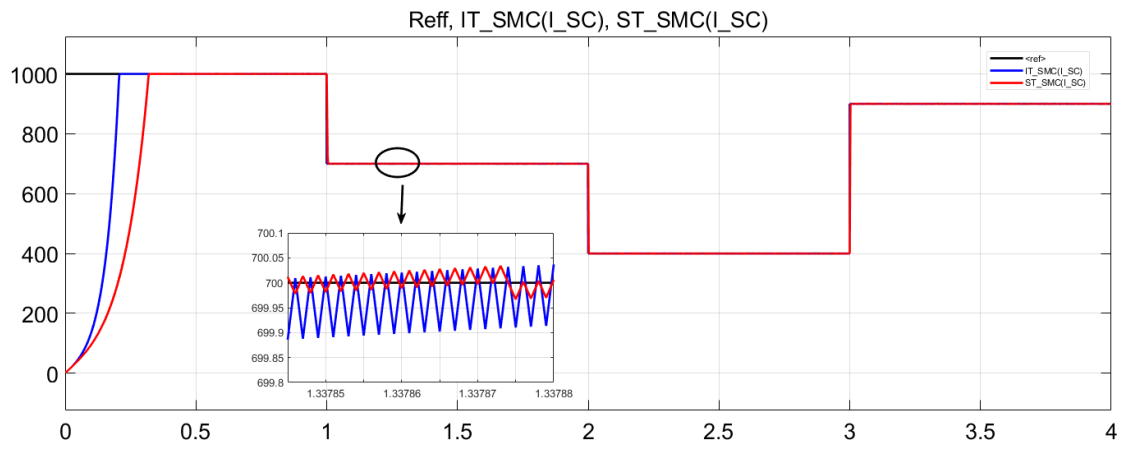


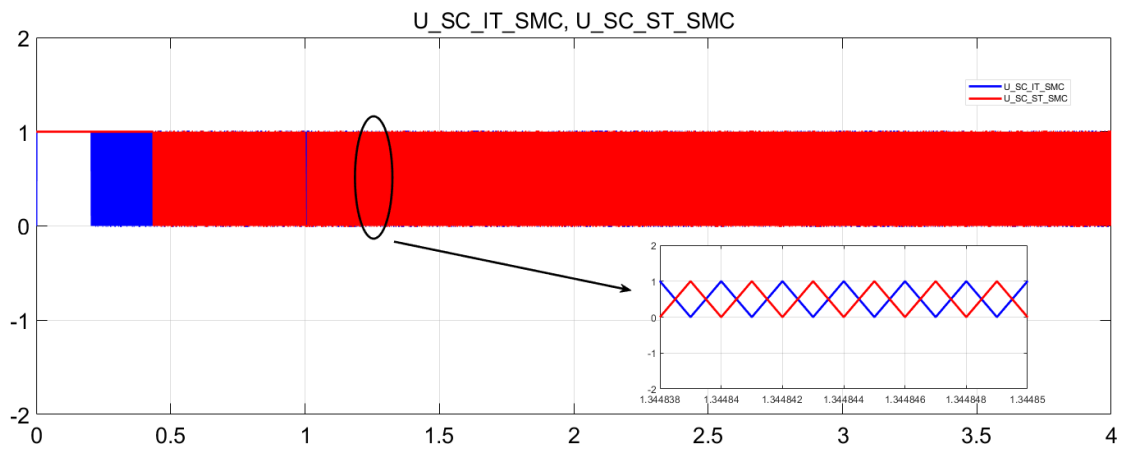**Figure 6.2:** I PV comparison between ITSMC and STSMC



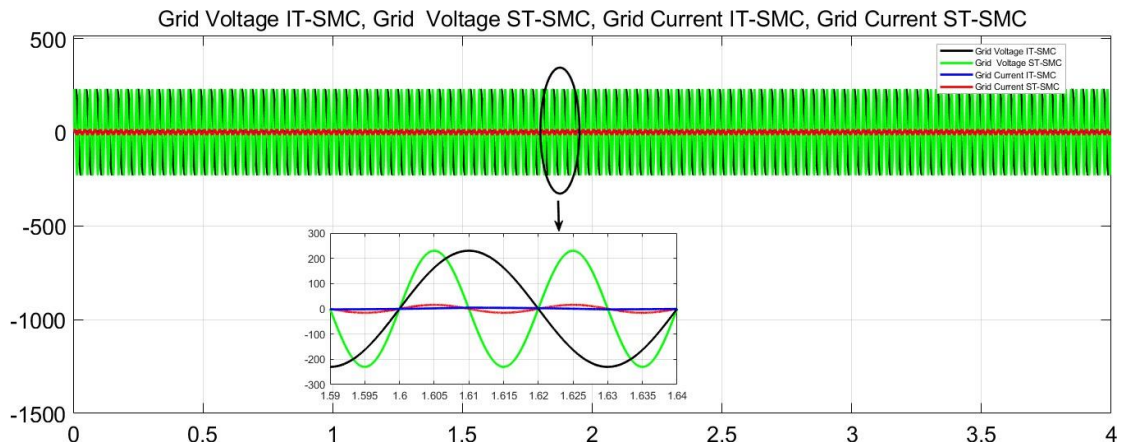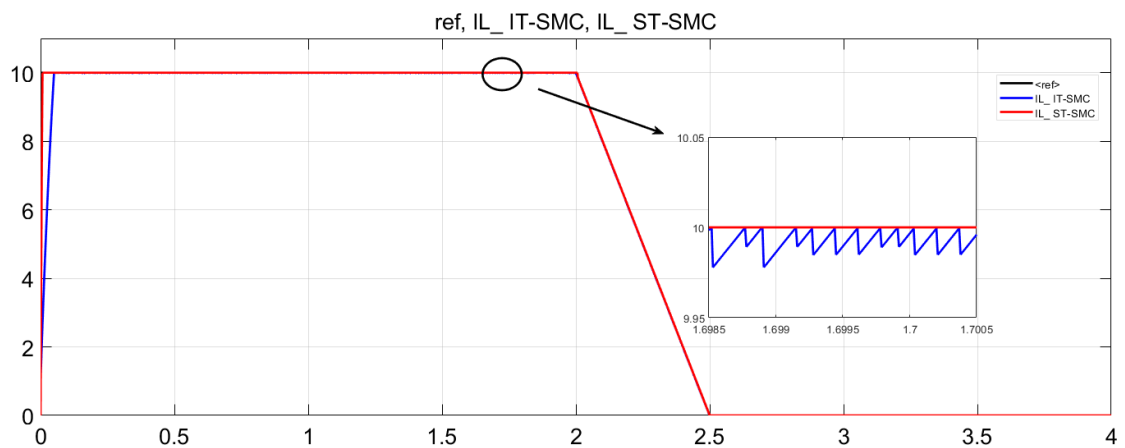**Figure 6.3:** U PV comparison between ITSMC and STSMC

**Figure 6.4:** I SC comparison between ITSMC and STSMC



**Figure 6.5:** U SC comparison between ITSMC and STSMC

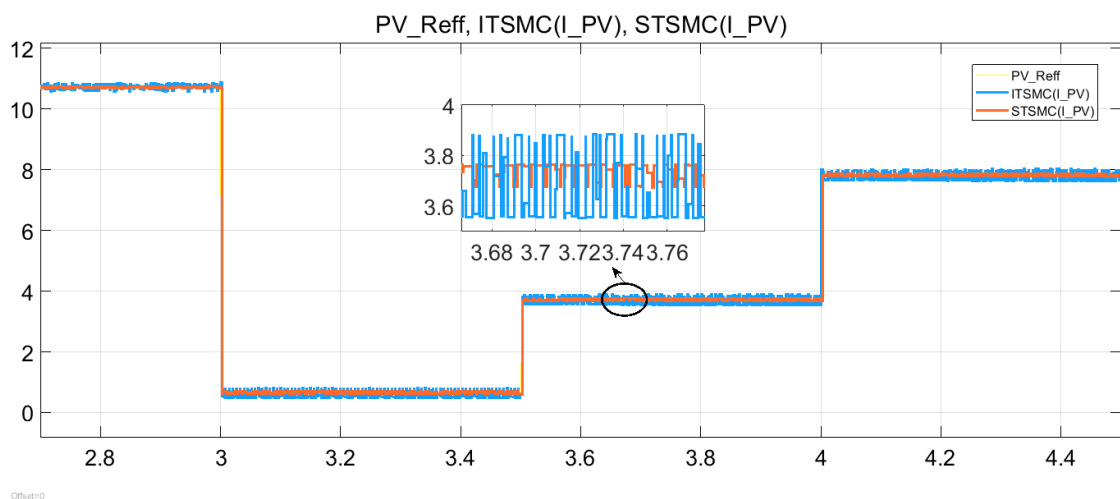**Figure 6.6:** Grid Voltage and Current comparison between ITSMC and STSMC



**Figure 6.7:** I Bat comparison between ITSMC and STSMC

Battery current of the proposed controllers in Eq. (51 and 95) has been simulated in the same environment along with the comparison to verify the performance and tracking of battery current. Fig. 6.7 shows the battery current generated against the reference current.

# Hardware-in-the-loop

Hardware-in-the-Loop (HIL) is a testing and simulation method widely used in engineering and automation [17]. It involves establishing a closed-loop connection between a physical system or component (hardware) and a computer-based simulation environment (software). This enables comprehensive testing and evaluation of the hardware's performance under various conditions by allowing real-time interaction between the device and the simulated environment. The hardware reacts to inputs from the simulation, and the outputs are recorded and fed back into the simulation environment. This closed-loop interaction between the hardware and the simulation enables realistic testing of the hardware's behavior, performance, and robustness [18].

To assess the resilience of the proposed methods, a discrete version of a sinusoidal disturbance with a varying amplitude over time is introduced. The simulation and Hardware-in-the-Loop (HIL) trajectories of the photovoltaic (PV) current are shown in Figure 13, demonstrating successful tracking of the desired reference trajectory. Additionally, Figures 14 and 15 illustrate the trajectories of the supercapacitor (SC) and grid voltage and current, which exhibit similar behavior. Notably, the SC trajectory appears to be more resilient to sinusoidal time-varying disturbances. Furthermore, Figure 16 presents the experimental response of the proposed controllers for battery current [19]. It is worth mentioning that the experimental results depicted in Figures 14 to 18 demonstrate minimal oscillations in the HIL trajectories of the proposed controllers for PV, SC, grid, and battery.
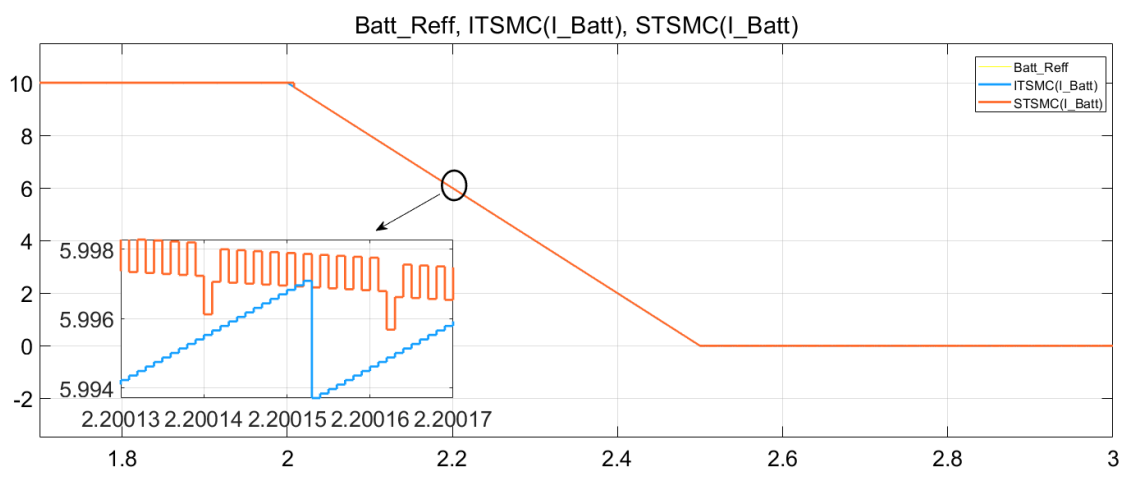
**Figure 7.1:** Responce of I PV comparison between ITSMC and STSMC
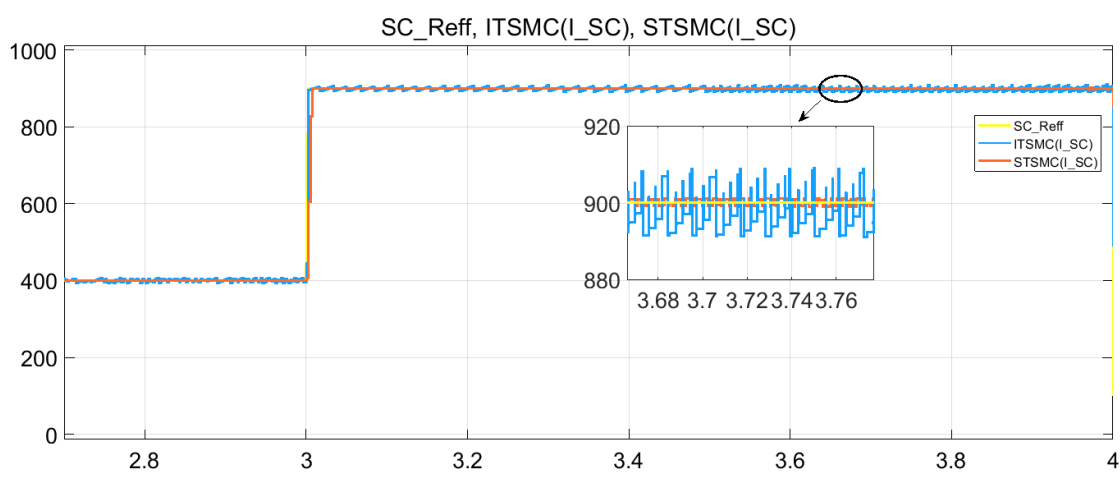


**Figure 7.2:** Responce of I SC comparison between ITSMC and STSMC
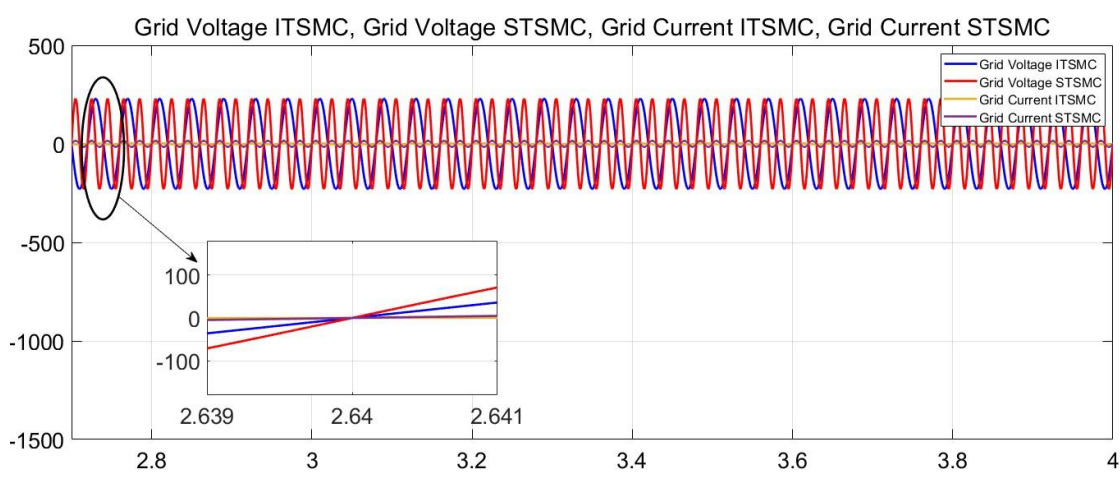


**Figure 7.3:** Responce Grid Voltage and Current comparison between ITSMC and STSMC

36

**Figure 7.4:** Responce of I Bat comparison between ITSMC and STSMC

# Conclusion and Future Work

This research article presents a comprehensive study on the integration of renewable energy sources, specifically photovoltaic (PV) systems, with an energy storage system comprising batteries and supercapacitors. The main objective is to effectively control the power sources, ensuring that they operate at their maximum power points and maintain a balanced power flow between the renewable energy sources and the energy storage system. To achieve this goal, supertwisting sliding mode controllers and integral terminal sliding mode controllers were implemented. These controllers facilitate efficient power management and meet the load requirements. The stability of the entire system was rigorously verified using Lyapunov analysis.

The proposed controllers, along with the energy management system, were extensively simulated in MATLAB/Simulink to assess the performance of the integrated framework. A comparative analysis with other existing controllers demonstrated that the proposed supertwisting sliding mode controllers outperformed them in terms of regulating the DC bus voltage and providing superior transient responses. Furthermore, hardware-in-the-loop experiments were conducted to validate the efficacy of the controllers. The experiments showed that the energy storage system effectively supported the renewable energy sources during high load demands, thus extending their lifespan.

In the future, this research can be extended in several directions. One potential avenue is the integration of additional energy sources, such as proton exchange membrane fuel cells, to reduce dependence on the energy storage system and further enhance the reliability of the overall system. Additionally, exploring grid-connected modes and designing an energy management system using various control algorithms could be beneficial to

maintain optimal power flow between the renewable energy sources, energy storage system, and the grid. Moreover, investigating advanced control techniques and optimization algorithms could lead to even more robust and efficient power management strategies for renewable energy integration. Overall, these future extensions can contribute to the development of more sustainable and reliable energy systems.

# References

[1] Syeda Shafia Zehra, Aqeel Ur Rahman, Hammad Armghan, Iftikhar Ahmad, and Umme Ammara. Artificial intelligence-based nonlinear control of renewable energies and storage system in a dc microgrid. *ISA transactions*, 121:217–231, 2022.

[2] David Coup. Toyota's approach to alternative technology vehicles: The power of diversification strategies. *Corporate Environmental Strategy*, 6(3):258–269, 1999.

[3] Rolf D Reitz, H Ogawa, R Payri, T Fansler, S Kokjohn, Y Moriyoshi, AK Agarwal, D Arcoumanis, D Assanis, C Bae, et al. Ijer editorial: The future of the internal combustion engine, 2020.

[4] Xuewei Pan, Hongqi Li, Yitao Liu, Tianyang Zhao, Chenchen Ju, and Akshay Kumar Rathore. An overview and comprehensive comparative evaluation of current-fed-isolated-bidirectional dc/dc converter. *IEEE Transactions on Power Electronics*, 35(3):2737–2763, 2019.

[5] Kulsoom Fatima, Ahmad Faiz Minai, and Hasmat Malik. Intelligent approach-based maximum power point tracking for renewable energy system: a review. *Intelligent Data Analytics for Power and Energy Systems*, pages 373–405, 2022.

[6] Ijaz Ahmed, Iftikhar Ahmad, Shahzad Ahmed, and Hafiz Mian Muhammad Adil. Robust nonlinear control of battery electric vehicle charger in grid to vehicle applications. *Journal of Energy Storage*, 42:103039, 2021.

[7] Asad Abbas, Iftikhar Ahmad, and Shahzad Ahmed. Barrier function-based adaptive terminal sliding mode control of plug-in hybrid electric vehicle with saturated control actions. *Journal of Energy Storage*, 65:107254, 2023.

*[8]* Attaphol Phimphui and Uthane Supatti. V2g and g2v using interleaved converter for a single-phase onboard bidirectional charger. In *2019 IEEE Transportation*

*Electrification Conference and Expo, Asia-Pacific (ITEC Asia-Pacific)*, pages 1–5. IEEE, 2019.

[9] Ramon Zamora and Anurag K Srivastava. Energy management and control algorithms for integration of energy storage within microgrid. In *2014 IEEE 23rd International Symposium on Industrial Electronics (ISIE)*, pages 1805–1810. IEEE, 2014.

[10] Luis F Grisales-Noreña, Oscar Danilo Montoya, and Carlos Andrés Ramos-Paja. An energy management system for optimal operation of bss in dc distributed generation environments based on a parallel pso algorithm. *Journal of Energy Storage*, 29: 101488, 2020.

[11] Naghmash Ali, Zhizhen Liu, Hammad Armghan, Iftikhar Ahmad, and Yanjin Hou. Lcc-s-based integral terminal sliding mode controller for a hybrid energy storage system using a wireless power system. *Energies*, 14(6):1693, 2021.

[12] Razieh Khanaki, Mohd Amran Mohd Radzi, and Mohammad Hamiruce Marhaban. Artificial neural network based maximum power point tracking controller for photovoltaic standalone system. *International Journal of Green Energy*, 13(3):283–291, 2016.

[13] Ijaz Ahmed, Muhammad Adnan, Mansoor Ali, and Georges Kaddoum. Supertwisting sliding mode controller for grid-to-vehicle and vehicle-to-grid battery electric vehicle charger. *Journal of Energy Storage*, 70:107914, 2023.

[14] Fayez FM El-Sousy, Mahmoud M Amin, and Osama A Mohammed. Robust adaptive neural network tracking control with optimized super-twisting sliding-mode technique for induction motor drive system. *IEEE Transactions on Industry Applications*, 58(3):4134–4157, 2022.

[15] K Punitha, D Devaraj, and S Sakthivel. Artificial neural network based modified incremental conductance algorithm for maximum power point tracking in photovoltaic system under partial shading conditions. *Energy*, 62:330–340, 2013.

[16] Amir Seyyedabbasi and Farzad Kiani. I-gwo and ex-gwo: improved algorithms of the grey wolf optimizer to solve global optimization problems. *Engineering with Computers*, 37(1):509–532, 2021.

[17] Fangming Gu, William S Harrison, Dawn M Tilbury, and Chengyin Yuan. Hardware-in-the-loop for manufacturing automation control: Current status and identified needs. In *2007 IEEE International Conference on Automation Science and Engineering*, pages 1105–1110. IEEE, 2007.

[18] Rolf Isermann, Jochen Schaffnit, and Stefan Sinsel. Hardware-in-the-loop simulation for the design and testing of engine-control systems. *Control Engineering Practice*, 7(5):643–653, 1999.

[19] Oliver König, Christoph Hametner, Günter Prochart, and Stefan Jakubek. Battery emulation for power-hil using local model networks and robust impedance control. *IEEE Transactions on Industrial Electronics*, 61(2):943–955, 2013.